Physica A 465 (2017) 75–90

Contents lists available at ScienceDirect

Physica A

journal homepage: www.elsevier.com/locate/physa

Coupling detrended fluctuation analysis for multiple warehouse-out behavioral sequences

Can-Zhong Yao [a,*], Ji-Nan Lin [b], Xu-Zhou Zheng [a]

[a] School of Economics and Commerce, South China University of Technology, Guangzhou, 510006, China
[b] Department of Economics, The Chinese University of Hong Kong, Hong Kong

HIGHLIGHTS

- Warehouse-out behaviors exhibit coupling multifractal characteristics.
- The fat-tail distribution contributes more to affecting behavioral dynamics features.
- The long-term memory of rebar will be more influential than that of wire rod.
- Significant coupling multifractal features emerged within time scale interval.

ARTICLE INFO

Article history:
Received 1 May 2016
Received in revised form 24 July 2016
Available online 13 August 2016

Keywords:
CDFA
Logistics system
Multifractal
MMA
Fat-tail distribution
Non-linear coupling relationship

ABSTRACT

Interaction patterns among different warehouses could make the warehouse-out behavioral sequences less predictable. We firstly take a coupling detrended fluctuation analysis on the warehouse-out quantity, and find that the multivariate sequences exhibit significant coupling multifractal characteristics regardless of the types of steel products. Secondly, we track the sources of multifractal warehouse-out sequences by shuffling and surrogating original ones, and we find that fat-tail distribution contributes more to multifractal features than the long-term memory, regardless of types of steel products. From perspective of warehouse contribution, some warehouses steadily contribute more to multifractal than other warehouses. Finally, based on multiscale multifractal analysis, we propose Hurst surface structure to investigate coupling multifractal, and show that multiple behavioral sequences exhibit significant coupling multifractal features that emerge and usually be restricted within relatively greater time scale interval.

1. Introduction

Mining of human behavioral data uncover a new realm of behavior interpretation and mechanism design. Beginning with human behavior dynamics, the burst feature and power law of behavioral inter-event time distribution [1], as well as the exponential spatial distance distribution of transportation behaviors [2], had received increasing attention. And some of experts characterized emergence of human behaviors by scaling laws [3–5]. Besides, large-scale behavioral data directly supplemented some sociological and social governance issues. For instance, based on online community dataset of Tencent QQ, You et al. [6] studied younger trend of online community, and size of social group and inner interaction with respect to age and gender.

* Corresponding author.
E-mail address: ycz20120911@gmail.com (C.-Z. Yao).

http://dx.doi.org/10.1016/j.physa.2016.08.016
0378-4371/

Yao et al. [7] researched on large-scale warehouse-out behaviors of logistics base, proposed the temporal scale scaling law of commercial individuals and groups, and further discussed the factors that determine the head, middle part and tail of inter-event time distribution. Based on visibility graph algorithm and Hurst exponent, they revealed the fractals features, and primarily demonstrated warehouse-out quantity was both determined by business cycle and systemic persistence. Further, the authors [8] also applied MF-DCCA and MF-DMA algorithms into characterizing cross-correlation multifractal of warehouse-out behaviors among warehouses and products, supplementing insights of cross-correlation of warehouses, products and factors of warehouse-out behaviors persistence. However, still few efforts have been devoted to detecting relationship of multiple sequences and understanding warehouse-out mechanism, especially on interactions between individual and the corresponding rest of group. This work is aiming to comprehensively reveal global behavioral features of warehouse-out system of multiple sequences, and propose a theoretical foundation for behavior-based logistics system optimization.

For origins of multifractal, Zhou [9] systematically studied the components of multifractality in financial returns based on shuffled and surrogated data of DJIA, and found fat-tail distribution plays a major role while temporal structure (linear correlation and nonlinearity) plays the minor one. Further based on partition function approach of multifractal analysis, Zhou [10] showed there is a finite-size effect in the detection of multifractality, and the effective multifractality can be decomposed into the probability distribution component, and the nonlinearity component.

Recently increasing methods are proposed to efficiently detect the multifractal property of multiple time series. DFA proposed by Peng et al. [11] and MF-DFA proposed by Kantelhardt et al. [12] accelerated the application of multifractal theory into time series, and promoted works in financial field on monofractal and multifractal prices time series analysis such as stock market prices [13], future market [14], exchange market [15], oil price [16], asset returns [17], etc.

In 2008, as to multifractal property on cross-correlation, Podobnik and Stanley [18] proposed a detrended cross-correlation analysis, and Zhou [19] extended it into multifractal cross-correlation analysis (MF-DCCA) based on DFA algorithm, and applied it into the analysis of two non-stationary signals. For joint multifractal measure, Meneveau et al. [20] discussed the extension of multifractal formalism from single variable into multivariate measure, which tended to be more useful for characterizing joint log-normal and joint binomial distributions. Wang et al. [21] proposed a new multifractal cross-correlation analysis based on statistical moments (MFSMXA) and applied into volatility series of DJIA and NASDAQ, with better performance compared with conventional multifractal detrending moving average cross correlation analysis (MFXDMA). Based on partition function approach with two moment orders, Xie et al. [22] analytically studied the property of joint multifractal analysis, and applied this new method MF-X-PF (p, q) to multifractal binomial measures. Owieimka et al. [23] proposed a new algorithm called multifractal cross-correlation analysis (MFCCA) to better describe multiscale cross-correlations between two time series than existing MF-DXA. Qian et al. [24] proposed detrended partial cross-correlation analysis (DPXA) to better study intrinsic power-law cross correlations between two nonstationary time series after removing the effects of their common forces.

DFA-based models have also been supplemented by works of correlation coefficients and regression framework. Zebende [25] proposed the DCCA cross-correlation coefficient to quantify the level of cross-correlation based on DFA and DCCA method, which had been proved to be successful in identifying both positive and negative cross-correlations of nonstationary time series. Kwapie et al. [26] introduced a new coefficient other than the existing detrended cross-correlation coefficient, which is not only able to quantify the strength of correlations but also identify the range of detrended fluctuation amplitudes that are correlated in two signals. To correctly detect cross-correlation beyond the influence of autocorrelation, Balocchi et al. [27] proposed the use of σ DCCA to quantify the degree of coupling between series. Kristoufek [28] investigated the ability of DCCA coefficient in measuring cross-correlation based on Monte Carlo simulation, and found it dominates the Pearson coefficient for nonstationary series. Further, Kristoufek [29] introduced DMCA coefficient based on moving-average cross-correlation analysis (DMCA), and found DMCA coefficient detects true correlation regardless of nonstationary level. The author [30] had also done great works in proposing a framework to combine detrended fluctuation analysis with standard regression methodology: improve standard least square regression by DFA-based regression with some new estimators.

Alessio et al. [31] first figured out a new multifractal detection method named detrending moving average analysis (DMA), which had been developed into MF-DMA [32]. It is worth mentioning that based on MF-DMA algorithm by Gu and Zhou [32], Jiang and Zhou [33] further proposed a robust method of multifractal detrending moving average cross-correlation analysis (MF-X-DMA). They tested three algorithms of centered, forward and backward MF-X-DMA, and found they outperformed the MF-X-DFA. Based on height–height correlation analysis, Kristoufek [34] carried out the multifractal height cross-correlation analysis (MF-HXA) to detect cross-correlation and multifractal of bivariate signals.

Gieratowski et al. [35] introduced a new method of multiscale multifractal analysis (MMA) based on time scale. They proposed sliding fitting windows to cover all ranges of scale s and obtain a series of overlapping windows, and then calculate the q order fluctuation function $F_q(s)$ of each point within windows. With this method, observing approximately continuous change process of $H_{xy}(q)$ with respect to scale s is available, and the process can be mapped into a surface about $H_{xy}(q, s)$. Gieratowski et al. [36] again applied MMA algorithm into studying the complex fluctuation of human fetal heart rate variability. Wang et al. [37] uncovered the complex structure of traffic sequences, and found MMA algorithm can extract more information than MF-DFA algorithm of fixed time scale. Further they demonstrated that the multifractal property of traffic sequences is rooted in both fatter probability density function and the correlation. Shi et al. [38] extended MMA into DCCA algorithm and proposed the multiscale multifractal detrended cross-correlation analysis (MM-DCCA), further

they applied it to financial time series and verified that MMA algorithm can simultaneously characterize monofractal and multifractal in a wider time scale range, without any assumption on fixed time scale. Yin et al. [39] applied MM-DCCA method into traffic flow sequences, and studied the correlative period of weekends and weekdays. Lin et al. [40] proposed a new MMA-based method DH-HMA, which can provide more stable and reliable characterization of scale, and studied power-law artificial data and 6 groups of stock market data. Results showed that stronger multifractal was found in Chinese market. Based on MM-DCCA model, Lin et al. [41] studied the multiscale multifractal property of Chinese and American stock markets based on MM-DCCA algorithm, and further operated principle component analysis for similarity of stock market dynamics.

Fruitful state-of-art works have been achieved on the shoulder of MMA models; however, most of them are two sequences and on fixed time scale. Therefore, we apply CDFA model to study multiple behavioral sequences and analyze its characteristics of multifractal under different time scales. Our work is the initial attempt to combine coupling detrended multifractal analysis with multiscale multifractal analysis, and to apply to warehouse-out logistics system. By empirically uncovering complex dynamics among multiple behavioral sequences, we shed light on the enhancement of real-world schedule and operation.

2. Multifractal of multiple sequences

2.1. Characteristics of coupling multifractal

According to literature [42], assuming n warehouse-out quantity time series with length N denoted $x_t^1, \ldots, x_t^j, \ldots, x_t^n$, and t means tth member of them.

- Construct cumulative sequences as:

$$X^j(i) = \sum_{t=1}^{i} (x_t^j - \overline{x_t^j}), \quad i = 1, 2, \ldots, N;\ j = 1, 2, \ldots, n \tag{1}$$

where $\overline{x_t^j} = \frac{1}{N}\sum_{t=1}^{N} x_t^j$.

- Divide each cumulative sequence $X_j(i)$ into $N_s = int\left(\frac{N}{s}\right)$ non-overlapping integer segments with length s. Since most of length of sequences are not multiples of the considered time scale s, we need to repeat this procedure starting from the end of time series. Therefore we may obtain $2N_s$ segments. Then we fit the each trend function $x_v^j(i)$, $v = 1, 2, \ldots, 2N_s$ of $2N_s$ segments, and calculate the detrended multivariate function as,

$$F_v(s) = \frac{1}{s}\sum_{i=1}^{s}\prod_{j=1}^{n}\left|X^j\left[(v-1)s+i\right] - x_v^j(i)\right|, \quad v = 1, \ldots, N_s \tag{2}$$

$$F_v(s) = \frac{1}{s}\sum_{i=1}^{s}\prod_{j=1}^{n}\left|X^j\left[N-(v-N_s)s+i\right] - x_v^j(i)\right|, \quad v = N_s+1, \ldots, 2N_s. \tag{3}$$

- Compute the q order fluctuation function:

$$F_v(s) = \begin{cases} \left\{\dfrac{1}{2N_s}\displaystyle\sum_{v=1}^{2N_s}\left[F_v(s)\right]^{\frac{q}{n}}\right\}^{\frac{1}{q}}, & q \neq 0 \\ \exp\left\{\dfrac{1}{2nN_s}\displaystyle\sum_{v=1}^{2N_s}\ln\left[F_v(s)\right]\right\}, & q = 0. \end{cases} \tag{4}$$

- If the warehouse-out quantity time series $x_t^1, \ldots, x_t^j, \ldots, x_t^n$ exhibit long-term power-law correlation, the $F_{x_t^1,\ldots,x_t^j,\ldots,x_t^n}(q, s)$ will increase as a power law with respect to s. For lots of s,

$$F_{x_t^1,\ldots,x_t^j,\ldots,x_t^n}(q, s) \sim s^{h_{x_t^1,\ldots,x_t^j,\ldots,x_t^n}(q)} \tag{5}$$

where $h_{x_t^1,\ldots,x_t^j,\ldots,x_t^n}(q)$ is the generalized Hurst exponent of coupling relationship of warehouse-out quantity time series $x_t^1, \ldots, x_t^j, \ldots, x_t^n$. If $h_{x_t^1,\ldots,x_t^j,\ldots,x_t^n}(q) > 0.5$, for a given q, there is long-term memory among the coupling relationship of warehouse-out quantity time series $x_t^1, \ldots, x_t^j, \ldots, x_t^n$. If $h_{x_t^1,\ldots,x_t^j,\ldots,x_t^n}(q) < 0.5$, for a given q, there is an anti-persistent property among the coupling relationship of warehouse-out quantity time series $x_t^1, \ldots, x_t^j, \ldots, x_t^n$. If $h_{x_t^1,\ldots,x_t^j,\ldots,x_t^n}(q) = 0.5$, for a given q, there is no coupling relationship of warehouse-out quantity time series or they are random-walk time series $x_t^1, \ldots, x_t^j, \ldots, x_t^n$. When $q > 0$, $h_{x_t^1,\ldots,x_t^j,\ldots,x_t^n}(q)$ characterize the scaling behaviors of n warehouse-out

quantity time series under large-scale fluctuation. When $q < 0$, $h_{x_t^1,\ldots,x_t^j,\ldots,x_t^n}(q)$ characterize the scaling behaviors of n warehouse-out quantity time series under small-scale fluctuation. The dependence of $h_{x_t^1,\ldots,x_t^j,\ldots,x_t^n}(q)$ on q indicates the presence of multifractal in coupling relationship of n warehouse-out quantity time series. However, the independence of $h_{x_t^1,\ldots,x_t^j,\ldots,x_t^n}(q)$ and q means monofractal or no fractal in coupling relationship of n warehouse-out quantity time series.

- According to work of Shadkhoo et al. [43], we can determine the parameters of multifractal spectrum and the relationship of $\tau_{x_t^1,\ldots,x_t^j,\ldots,x_t^n}$ and q:

$$\tau_{x_t^1,\ldots,x_t^j,\ldots,x_t^n} = qh_{x_t^1,\ldots,x_t^j,\ldots,x_t^n}(q) - 1 \tag{6}$$

$$\begin{cases} \alpha = \dfrac{\mathrm{d}\tau_{x_t^1,\ldots,x_t^j,\ldots,x_t^n}(q)}{\mathrm{d}q} \\ f(\alpha) = \alpha q - \tau_{x_t^1,\ldots,x_t^j,\ldots,x_t^n}(q). \end{cases} \tag{7}$$

2.2. Source of coupling multifractal

Generally speaking, coupling multifractal is rooted in three sources: caused only by long-term memory of large-scale fluctuation and small-scale fluctuation; only from the fat-tail distribution of fluctuation; both resulted from long-term memory and fat-tail distribution of fluctuation. In order to explore the source of coupling multifractal in warehouse-out system and further determine the contribution of both sources, this paper will shuffle and surrogate the original time series.

The main steps of shuffling [44] involve,

- Randomly generate a pair of integers (p, q), where $p \leq N$, $q \leq N$ (N represents the length of time series);
- Switch the position of pth data point and qth data point;
- Repeat the mentioned steps for $20N$ times to ensure completely shuffling.

The steps of surrogating [45] mainly cover,

- Perform Discrete Fourier Transform on time series;
- Randomly rotate the phase angle;
- Utilize Inverse Fourier Transform.

If the coupling multifractal becomes monofractal after shuffling, the source of coupling multifractal is mainly from long-term memory; if the coupling multifractal becomes monofractal after surrogating, the source of coupling multifractal is mainly from fat-tail probability distribution. If the coupling multifractal of time series still follows reduced multifractal property even after both shuffling and surrogating process, the coupling multifractal could jointly result from both long-term memory and fat-tail probability distribution.

Given that a coupling multifractal relationship is caused by both sources, we can primarily compare the strength of multifractal after shuffling or surrogating. If the strength of multifractal of shuffled data is greater than that of surrogated data, we can argue that the impact of fat tail distribution will be greater than that of long-term memory and vice versa.

2.3. Source contribution of coupling multifractal

Based on the *Chi Squares* statistic proposed by Hedayatifar et al. [42], we quantify the contribution of long-term memory or fat-tail probability distribution to coupling multifractal:

$$\chi^2_{\diamond}(Y) = \sum_{i=1}^{N_q} \frac{h(q_i) - h^Y_{\diamond}(q_i)}{\sigma(q_i)^2 + \sigma^Y_{\diamond}(q_i)^2} \tag{8}$$

$$\sigma(q) = \begin{cases} \left\{ \dfrac{1}{N} \displaystyle\sum_{i=1}^{N} \prod_{j=1}^{n} \left[X^j(i) - \overline{X^j} \right]^{\frac{q}{n}} \right\}^{\frac{1}{q}}, & q \neq 0 \\ \exp\left\{ \dfrac{1}{nN} \displaystyle\sum_{i=1}^{N} \ln \left[\prod_{j=1}^{n} (X^j(i) - \overline{X^j}) \right] \right\}, & q = 0 \end{cases} \tag{9}$$

where N_q represents the number of degrees of freedom; $h(q)$ is the generalized Hurst exponent of n sequences coupling multifractal; $h^Y_{\diamond}(q)$ is the generalized Hurst exponent of coupling multifractal of a shuffled or surrogated sequence Y and the rest $n-1$ original sequences. Similarly, $\sigma(q)$ is the generalized standard deviation of sequence coupling relationship, and $\sigma^Y_{\diamond}(q)$ is the generalized standard deviation of coupling multifractal of a shuffled or surrogated sequence Y and the rest $n-1$ original sequences. Higher $\chi^2_{\diamond}(Y)$ means higher degree of coupling between sequence Y and other sequences; i.e. the impact of multifractal of sequence Y on multifractal of n original sequences is greater.

Table 1
Basic statistics description for warehouse-out quantity of logistics system.

	Total amount of steel		YZ warehouse			BY warehouse			JS warehouse		
	Rebar	Wire rod	Rebar	Wire rod	Total	Rebar	Wire rod	Total	Rebar	Wire rod	Total
Observations	427 289	529 015	163 808	172 465	336 273	258 930	175 962	434 892	106 277	78 862	185 139
Mean	5747.248	5522.12	1949.116	2619.584	4568.7	2621.61	1812.546	4434.156	1176.522	1089.99	2266.512
Max	15 273.1	26 712.91	10 751.02	24 804.89	26 565.94	9337.05	5708.39	11 237.48	5365.775	6710.78	8354.22
Min	0	2.22	0	0	0	0	0	0	0	0	0
Standard deviation	2622.69	2626.789	1191.398	1421.662	2235.526	1519.068	917.759	2240.424	770.983	1127.413	1475.019
Skewness	0.141	0.623	1.368	2.627	0.941	0.486	0.45	0.217	1.044	1.737	0.904
Kurtosis	2.69	5.156	6.666	37.754	8.186	2.823	3.193	2.532	4.506	6.234	3.583
Jarque–Bera statistics	12.196	431.194	1455.087	85 913.69	2116.581	9337.05	59.006	28.325	461.04	1566.345	250.937

3. Data description

To recognize the patterns of the warehouse-out behaviors, we use the daily warehouse-out quantity records of steel products of a logistics from January 1*st*, 2009 to October 1*st*, 2013.

The specialized and large-scale base is composed of three warehouses YZ, JS and BY warehouses. In 2010, the capacity of the base grew up to 16 million tons, and it was the logistics service provider for many large enterprises like *Bao Steel, Tangshan Iron & Steel Company*, and *Guangzhou Honda*.

When analyzing coupling relationship, we focus on two aspects. First, we respectively study coupling multifractal of steel warehouse-out quantity of YZ, JS and BY warehouses. Second, owing to the differences of rebar and wire rod, we also analyze the coupling between these two products in each warehouse. The total warehouse-out quantity of steel is the sum of two types of products including rebar and wire rod.

Table 1 is the descriptive statistics results of all warehouse-out quantity sequences. As shown in Table 1, the JB statistic of each sequence is significantly greater than the critical value (the critical value under 1% significance level is 9.2103), which reveals the leptokurtie and fat-tailed features.

4. Coupling multifractal of product among multiple warehouses

4.1. Coupling multifractal of wire rod among warehouses

Fig. 1(a)–(d) show that the warehouse-out quantity sequences of wire rod among YZ, JS and BY warehouses exhibit coupling multifractal property. Therefore, from perspective of unique product of wire rod, the warehouse-out behaviors among warehouses cannot be considered independent, or be thought to be scheduled only based on business cycle and raw material price. The warehouse-out behaviors of wire rod follow autocorrelation multifractal, and reflect the self-persistent long-term correlation [7]. Additionally, the warehouse-out behaviors also follow cross-correlation multifractal [8], and further exhibit complex coupling multifractal property.

Fig. 1(a) shows that for different q, the fluctuation function can basically be fitted by a straight line under log–log coordinate. Referring to formula (5), the coupling multifractal of wire rod among warehouses tends to follow power-law coupling features. That means long-term memory of warehouse-out sequences of wire rod among warehouses; this kind of long-term memory interacts with each other, and causes the coupling fluctuation function to exhibit different fractal dimensions under different scales.

Results of Fig. 1(b) show that no matter $q > 0$ or $q < 0$, the generalized Hurst exponents are still above 0.5, revealing that the coupling relationship among warehouse-out behaviors of wire rod is self-persistent. Therefore no matter under large-scale fluctuation or small-scale fluctuation, the fluctuation of warehouse-out behavior of wire rod of a single warehouse will positively affect that of other two warehouses.

Furthermore, according to formula (6) and formula (7), we can obtain the multifractal scaling exponent and multifractal singular spectra function to characterize the coupling relationship of warehouse-out behaviors among warehouses. The multifractal singular spectra function in reality reflects the complex dynamics of warehouse-out system, and width of spectrum $\alpha = \alpha_{\max} - \alpha_{\min}$ can be used to measure the strength of multifractal in sequences as well as the absolute magnitude of warehouse-out fluctuation.

4.2. Coupling multifractal of rebar among warehouses

Similarly, from Fig. 2(a)–(d), we find the warehouse-out behaviors of rebar among YZ, JS and BY warehouses also follow coupling multifractal property.

Fig. 2(a) shows that for different q, the fluctuation function can basically be fitted by a straight line under log–log coordinate. Referring to formula (5), the coupling multifractal of rebar among warehouses tends to follow power-law

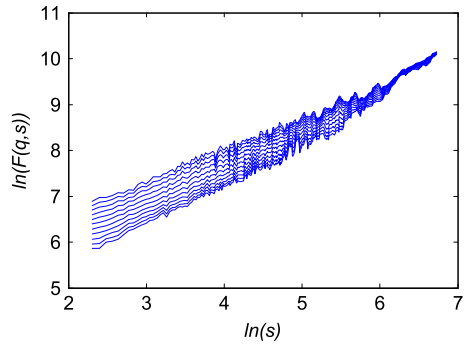

(a) $F(q, s) \sim s$.

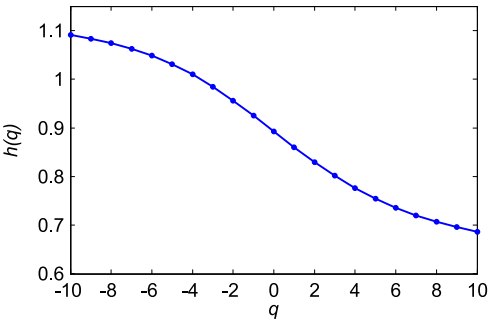

(b) $h(q) \sim q$.

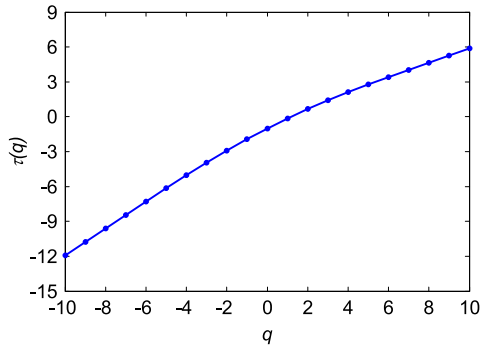

(c) $\tau(q) \sim q$.

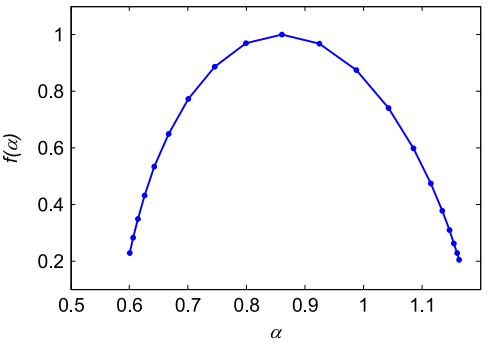

(d) $f(\alpha) \sim \alpha$.

Fig. 1. Graph of wire rod warehouse-out quantity coupling multifractal among YZ, JS and BY warehouses.

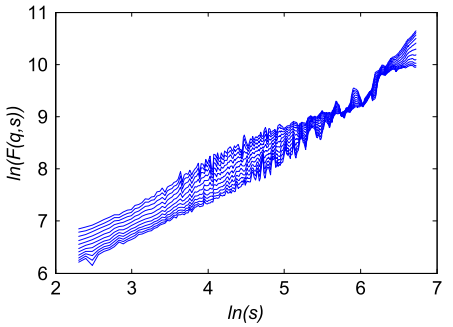

(a) $F(q, s) \sim s$.

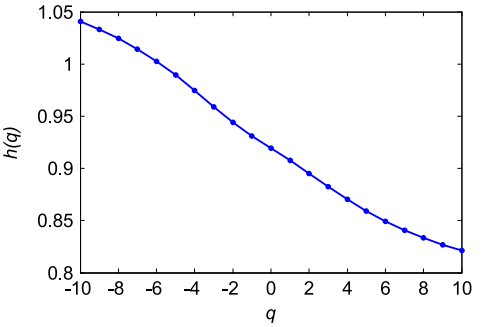

(b) $h(q) \sim q$.

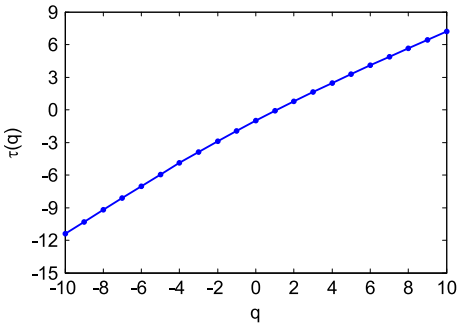

(c) $\tau(q) \sim q$.

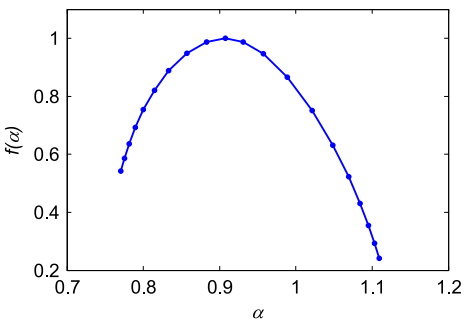

(d) $f(\alpha) \sim \alpha$.

Fig. 2. Graph of rebar warehouse-out quantity coupling multifractal among YZ, JS and BY warehouses.

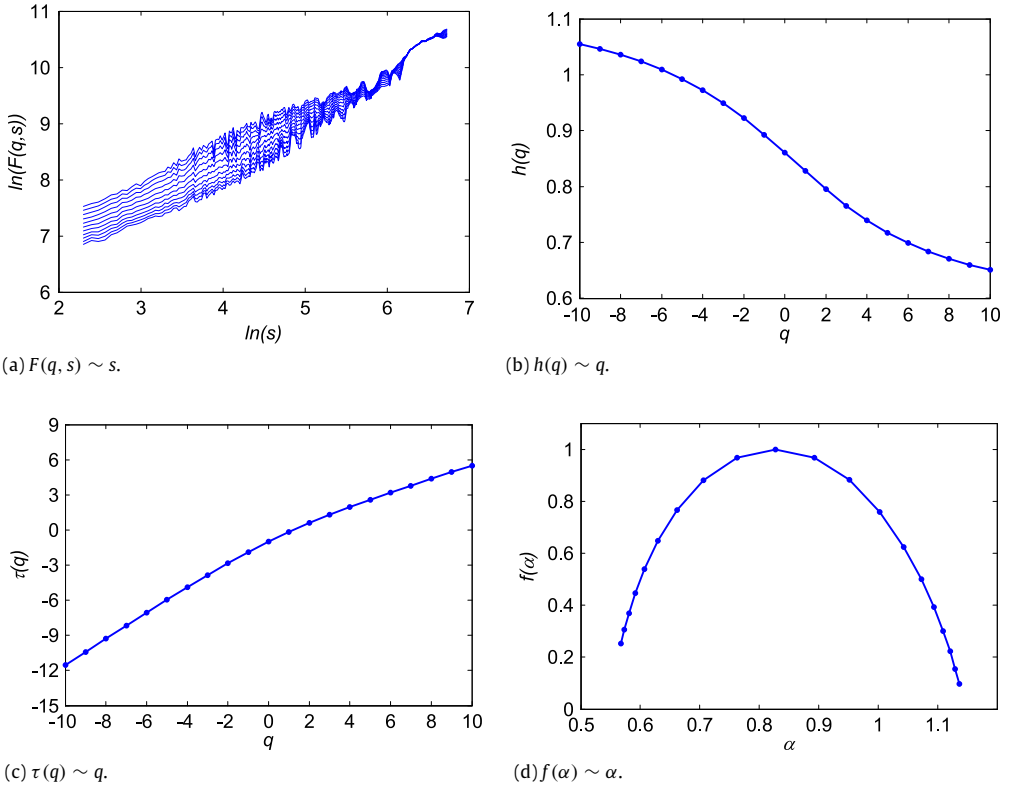

(a) $F(q, s) \sim s$. (b) $h(q) \sim q$.

(c) $\tau(q) \sim q$. (d) $f(\alpha) \sim \alpha$.

Fig. 3. Graph of total steel warehouse-out quantity coupling multifractal among YZ, JS and BY warehouses.

coupling features. That means warehouse-out sequences among warehouses would have long-term memory features; this kind of long-term memory interacts with each other, and causes the coupling fluctuation function to exhibit different fractal dimensions under different scales.

Results of Fig. 2(b) show that no matter $q > 0$ or $q < 0$, the generalized Hurst exponents are still above 0.5, revealing that the coupling relationship among warehouse-out behaviors of rebar is self-persistent. Therefore no matter under large-scale fluctuation or small-scale fluctuation, the fluctuation of warehouse-out behavior of rebar of a single warehouse will positively affect that of other two warehouses.

Additionally, by comparing Figs. 1(b) and 2(b), we observe that under different fluctuation, the strength of coupling multifractal of warehouse-out behaviors of rebar reduces from 1.05 to 0.8, while that of wire rod declines from 1.1 to 0.7.

There exists an intersection of multifractal strength of two products, when the fluctuation is less than the fluctuation of that intersection, the multifractal strength of wire rod will be greater than that of rebar; when the fluctuation is greater than the fluctuation of that intersection, the multifractal strength of rebar will be greater than that of wire rod.

4.3. Coupling multifractal of steel among warehouses

For a given time and a given warehouse, without specifying rebar and wire rod, instead we sum up both and regard as the overall steel warehouse-out quantity. The analysis is also carried out by operating a given sequence from one of three houses.

Similarly from Fig. 3(a)–(d), we find the warehouse-out behaviors of steel among YZ, JS and BY warehouses also follow coupling multifractal property.

Fig. 3(a) shows that for different q, the fluctuation function can basically be fitted by a straight line under log–log coordinate. Referring to formula (5), the coupling multifractal of rebar among warehouses tends to follow power-law coupling features. That means long-term memory of warehouse-out sequences of rebar among warehouses; this kind of long-term memory interacts with each other, and causes the coupling fluctuation function to exhibit different fractal dimensions under different scales.

Results of Fig. 3(b) show that no matter $q > 0$ or $q < 0$, the generalized Hurst exponents are still above 0.5, revealing that the coupling relationship among warehouse-out behaviors of rebar is self-persistent. Therefore no matter under large-scale fluctuation or small-scale fluctuation, the fluctuation of warehouse-out behavior of steel of a single warehouse will positively affect that of other two warehouses.

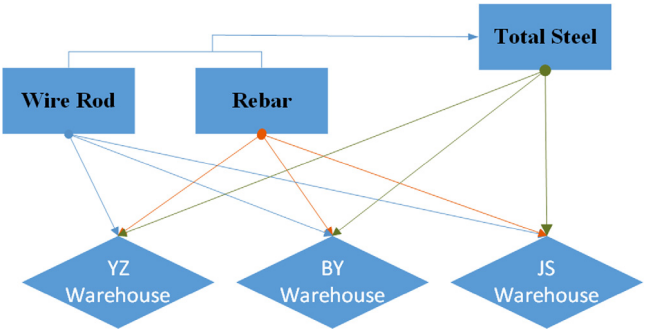

Fig. 4. Logic relationship of warehouse-product combination. Total steel is the sum of wire rod and rebar. Three warehouses are YZ, JS and BY, and for each warehouse, the products include both wire rod and rebar. For each product, warehouse-out behavior of each warehouse will affect that of rest two warehouses.

Additionally, by comparing Figs. 1(b), 2(b) and 3(b), we observe that under different fluctuation, the strength of coupling multifractal of warehouse-out behaviors of rebar reduces from 1.05 to 0.8; while that of wire rod declines from 1.1 to 0.7; steel reduces from 1.05 to 0.65. This reveals that if we do not specify rebar and wire rod and study the warehouse-out behavior from perspective of steel, the strength of coupling multifractal probably slightly decreases. This is because when we sum up two products at the same time, a part of strength of coupling multifractal of a single product will be offset, and makes the strength of coupling multifractal of steel decrease.

5. Contribution of a warehouse to coupling multifractal

In Section 3 we find that no matter for wire rod, rebar or steel, the coupling multifractal of warehouse-out behaviors among YZ, JS and BY warehouses is significant, revealing that probably the interaction of interdependence among warehouse-out behaviors follows long-term memory.

This section mainly utilizes the shuffle and surrogate procedure on original sequences, and determines the contribution of long-term memory or fat-tail probability distribution of a given sequence contributes more to the coupling multifractal.

In this analysis, we separate products into three types: wire rod, rebar and total steel. As for each product, we aim to divide the contribution of each warehouse (Fig. 4).

5.1. Wire rod

- **YZ warehouse**

  We shuffle and surrogate the original sequences of wire rod warehouse-out quantity in YZ warehouse, and study the contribution of long-term memory and fat-tail probability distribution of YZ warehouse to strength of coupling multifractal.

  In Fig. 5, we find both long-term memory and fat-tail probability distribution of YZ wire rod warehouse-out behavior affect the coupling multifractal of wire rod warehouse-out behaviors. As illustrated in Fig. 5, the strength of coupling multifractal after surrogate procedure of YZ is less than the strength of coupling multifractal after shuffle procedure of YZ. Therefore, we can infer that from perspective of contribution to coupling multifractal of wire rod, the fat-tail probability of YZ is greater than long-term memory of YZ.
- **JS warehouse**

  Similarly, we shuffle and surrogate the original sequences of wire rod warehouse-out quantity in JS warehouse, and study the contribution of long-term memory and fat-tail probability distribution of JS warehouse to strength of coupling multifractal.

  In Fig. 6, we find both long-term memory and fat-tail probability distribution of JS wire rod warehouse-out behavior affect the coupling multifractal of wire rod warehouse-out behaviors. As illustrated in Fig. 6, the strength of coupling multifractal after surrogate procedure of JS is less than the strength of coupling multifractal after shuffle procedure of JS. Therefore, we can infer that from perspective of contribution to coupling multifractal of wire rod, the fat-tail probability of JS is greater than long-term memory of JS.
- **BY warehouse**

  Similarly, we shuffle and surrogate the original sequences of wire rod warehouse-out quantity in BY warehouse, and study the contribution of long-term memory and fat-tail probability distribution of BY warehouse to strength of coupling multifractal.

  In Fig. 7, we find both long-term memory and fat-tail probability distribution of BY wire rod warehouse-out behavior affect the coupling multifractal of wire rod warehouse-out behaviors. As illustrated in Fig. 7, the strength of coupling multifractal after surrogate procedure of BY is greater than the strength of coupling multifractal after shuffle procedure

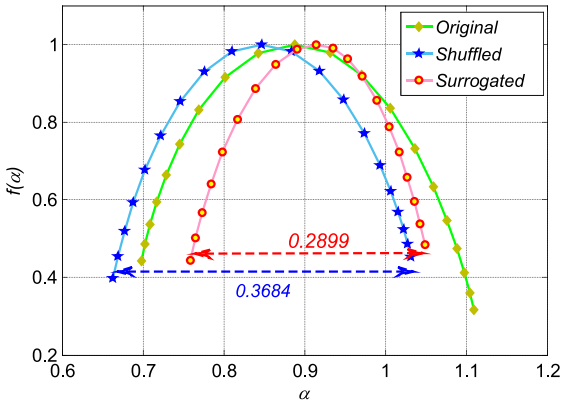

Fig. 5. $f(\alpha) \sim \alpha$ graph of wire rod warehouse-out quantity coupling multifractal among YZ, JS and BY warehouses with change of YZ.

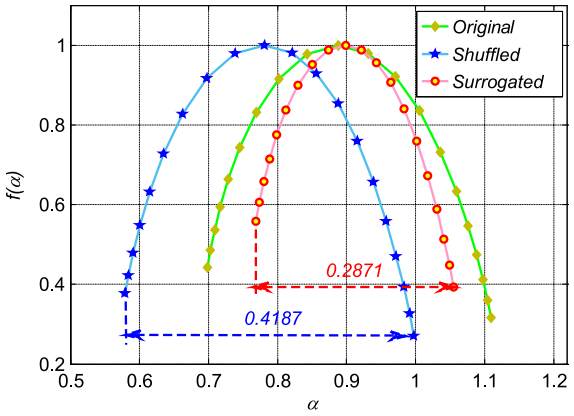

Fig. 6. $f(\alpha) \sim \alpha$ graph of wire rod warehouse-out quantity coupling multifractal among YZ, JS and BY warehouses with change of JS.

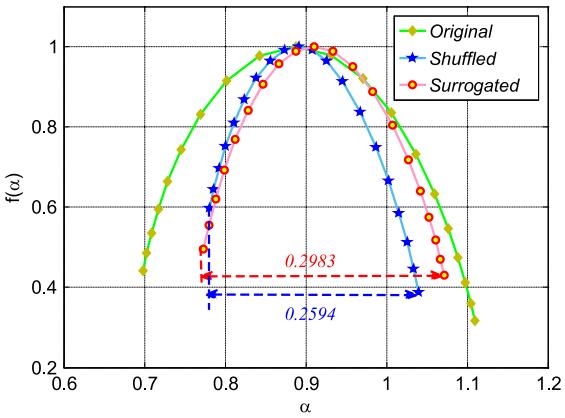

Fig. 7. $f(\alpha) \sim \alpha$ graph of wire rod warehouse-out quantity coupling multifractal among YZ, JS and BY warehouses with change of BY.

of BY. Therefore, we can infer that from perspective of contribution to coupling multifractal of wire rod, the fat-tail probability of BY is less than long-term memory of BY.

- **Comparison of warehouses**

The above study is mainly to extract the long-term memory or fat-tail features by each house. However, in order to rank the importance of three houses, we put $h(q)$ cures together with shuffled effect or surrogated effect.

Fig. 8(a) shows the generalized Hurst exponents of coupling multifractal by shuffling one of the warehouse-out behaviors from YZ, JS or BY warehouse. We can observe that the curve of shuffling JS warehouse is farthest from original CDFA curve, followed YZ and BY warehouses. Therefore, for contribution of long-term to coupling multifractal, JS warehouse can probably rank top, and is followed by YZ and BY warehouses.

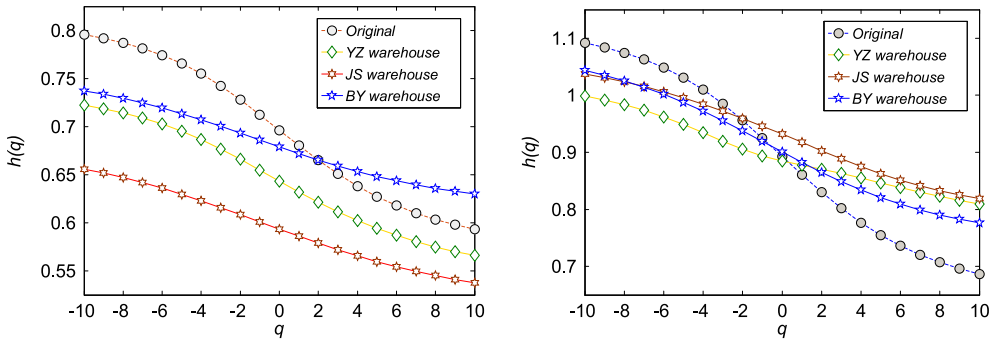

(a) Shuffled effect. (b) Surrogated effect.

Fig. 8. Wire rod warehouse-out quantity coupling multifractal among YZ, JS and BY warehouses.

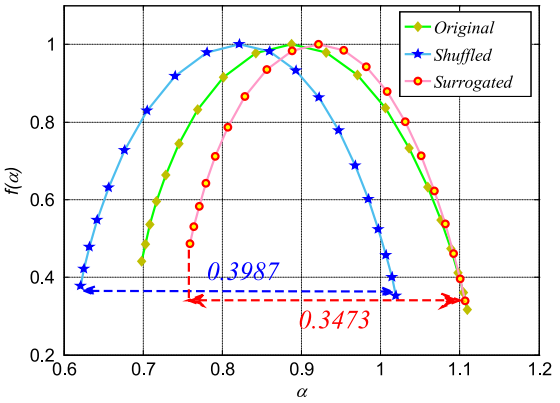

Fig. 9. $f(\alpha) \sim \alpha$ graph of rebar warehouse-out quantity coupling multifractal among YZ, JS and BY warehouses with change of YZ.

Fig. 8(b) shows the generalized Hurst exponents of coupling multifractal by surrogating one of the warehouse-out behaviors from YZ, JS or BY warehouse. Compared with Fig. 8(a), we find curves of surrogated sequences are all close to original CDFA curve. Therefore, compared with long-term memory, the differences of contribution of fat-tail distribution among warehouses are not significant.

5.2. Rebar

- **YZ warehouse**

  We shuffle and surrogate the original sequences of rebar warehouse-out quantity in YZ warehouse, and study the contribution of long-term memory and fat-tail probability distribution of YZ warehouse to strength of coupling multifractal.

  In Fig. 9, we find both long-term memory and fat-tail probability distribution of YZ rebar warehouse-out behavior affect the coupling multifractal of rebar warehouse-out behaviors. As illustrated in Fig. 9, the strength of coupling multifractal after surrogate procedure of YZ is less than the strength of coupling multifractal after shuffle procedure of YZ. Therefore, we can infer that from perspective of contribution to coupling multifractal of rebar, the fat-tail probability of YZ is greater than long-term memory of YZ, and the contribution of long-term memory is relatively tiny.
- **JS warehouse**

  Similarly, we shuffle and surrogate the original sequences of rebar warehouse-out quantity in JS warehouse, and study the contribution of long-term memory and fat-tail probability distribution of JS warehouse to strength of coupling multifractal.

  In Fig. 10, we find both long-term memory and fat-tail probability distribution of JS rebar warehouse-out behavior affect the coupling multifractal of rebar warehouse-out behaviors. As shown in Fig. 10, the strength of coupling multifractal after surrogate procedure of JS is less than the strength of coupling multifractal after shuffle procedure of JS. Therefore, we can infer that from perspective of contribution to coupling multifractal of wire rod, the fat-tail probability of JS is greater than long-term memory of JS.
- BY **Warehouse**

  Similarly, we shuffle and surrogate the original sequences of rebar warehouse-out quantity in BY warehouse, and study the contribution of long-term memory and fat-tail probability distribution of BY warehouse to strength of coupling multifractal.

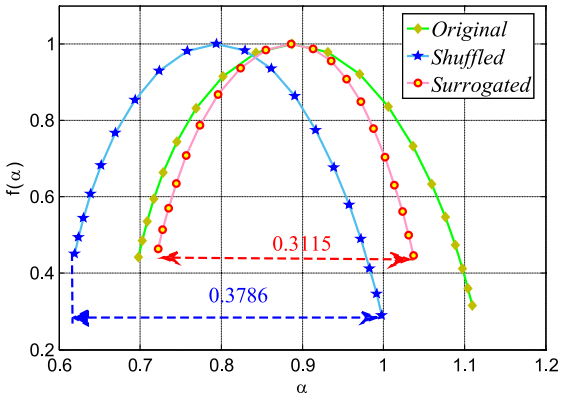

Fig. 10. $f(\alpha) \sim \alpha$ graph of rebar warehouse-out quantity coupling multifractal among YZ, JS and BY warehouses with change of JS.

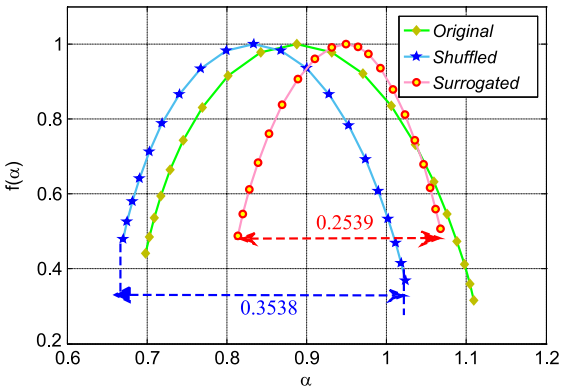

Fig. 11. $f(\alpha) \sim \alpha$ graph of rebar warehouse-out quantity coupling multifractal among YZ, JS and BY warehouses with change of BY.

In Fig. 11, we find both long-term memory and fat-tail probability distribution of BY rebar warehouse-out behavior affect the coupling multifractal of rebar warehouse-out behaviors. Shown in Fig. 11, the strength of coupling multifractal after surrogate procedure of BY is less than the strength of coupling multifractal after shuffle procedure of BY. Therefore, we can infer that from perspective of contribution to coupling multifractal of rebar, the fat-tail probability of BY is greater than long-term memory of BY.

- **Comparison of warehouses**

  Fig. 12(a) shows the generalized Hurst exponents of coupling multifractal by shuffling one of the warehouse-out behaviors from YZ, JS or BY warehouse. We can observe that the curve of shuffling JS warehouse is farthest from original CDFA curve, followed YZ and BY warehouses. Therefore, for contribution of long-term to coupling multifractal, JS warehouse can probably rank top, and is followed by YZ and BY warehouses. Fig. 12(b) shows the generalized Hurst exponents of coupling multifractal by surrogating one of the warehouse-out behaviors from YZ, JS or BY warehouse. Compared with Fig. 12(a), we find curves of surrogated sequences are all close to original CDFA curve. Therefore, compared with long-term memory, the differences of contribution of fat-tail distribution among warehouses are not significant. However, JS warehouse is still ranked top for influence of fat-tail distribution.

5.3. Steel product

Respectively, we shuffle and surrogate the original sequences of steel warehouse-out quantity in JS, YZ and BY warehouses, and to verify whether the long-term memory or the fat-tail probability distribution is the main contribution. The results exhibit that the fat-tail probability is greater than long-term memory regardless of the warehouses. Further, we also divide the warehouse-product into six groups, and reveal the main contribution factors by comparing the $h(q)$ values (Fig. 13).

Fig. 13(a) shows the generalized Hurst exponents of coupling multifractal by shuffling one of the warehouse-out behaviors from YZ, JS or BY warehouse of both rebar and wire rod products. We can observe that the curves of shuffling JS warehouse of rebar and wire rod are farthest from original CDFA curve, followed YZ-rebar, BY-rebar, YZ-wire rod and BY-wire rod. Therefore, for contribution of long-term to coupling multifractal, JS warehouse can probably rank top no matter for wire rod or rebar, and followed by YZ and BY warehouses. And for comparison of long-term memory of products, the influence of coupling multifractal of rebar is relatively greater than that of wire rod.

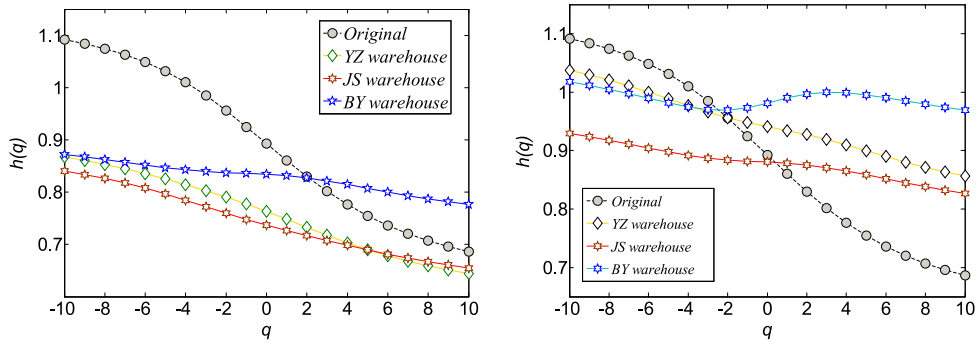

(a) Shuffled effect. (b) Surrogated effect.

Fig. 12. Rebar warehouse-out quantity coupling multifractal among YZ, JS and BY warehouses.

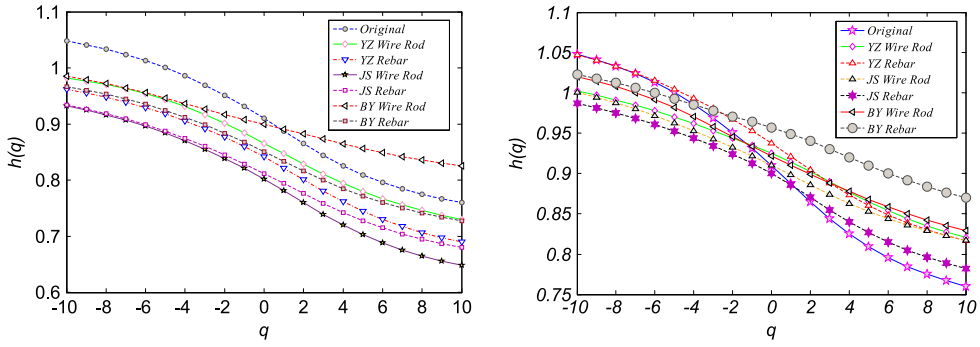

(a) Shuffled effect. (b) Surrogated effect.

Fig. 13. Wire rod and rebar warehouse-out quantity coupling multifractal among YZ, JS and BY warehouses.

Fig. 13(b) shows the generalized Hurst exponents of coupling multifractal by surrogating one of the warehouse-out behaviors from YZ, JS or BY warehouse of both rebar and wire rod products. We can observe that the curves of surrogating JS warehouse of rebar and wire rod are farthest from original CDFA curve, followed BY-wire rod, YZ-wire rod, YZ-rebar and BY-rebar. Therefore, for contribution of fat-tail distribution to coupling multifractal, JS warehouse can probably rank top no matter for wire rod or rebar, and followed by YZ and BY warehouses. The difference between YZ and BY warehouses and the difference between rebar and wire rod are not significant.

6. Hurst surface of multiscale coupling multifractal

In order to keep a constant width of sliding window in log–log coordinate, in reality we need to make the width of window exponentially increasing.

6.1. Introduction of sliding window

MMA algorithm is a kind of multifractal characterization by simultaneously incorporating time scale and fluctuation, and mapping them into a surface. To our knowledge, there is no precise range $h(q)$ to determine a monofractal. Therefore, uncovering the structure of $h(q)$ from different time scales will tend to be more informative.

Based on sliding windows, MMA algorithm [32] covered the fluctuation function $F(q, s)$ of all range of s, and proposed the Hurst surface $h(q, s)$, where s denotes time scale, q denotes parameter of multifractal. There are 4 important parameters in MMA algorithm: s, q, wl, sl. wl denotes the width of sliding windows, and sl denotes the length of sliding. These 4 parameters are defined in terms of intervals: $q = \left[q_{\min} : q_{\max}, q_{step}\right]$, $s = [s_{\min} : s_{\max}, s_{number}]$, $wl = \left[wl_{\min} : wl_{\max}, wl_{step}\right]$, $sl = \left[sl_{\min} : sl_{\max}, sl_{step}\right]$. For instance, $s = [20 : 2000, 30]$ represents that under logarithm coordinate, time scale increases from 20 to 2000 by 30.

It seems to be the appropriate choice of the range of scales s, for which the family of curves $F(q, s)$ should be calculated. A too large s results in the division of the time series into a too small number of windows. In turn, too small scales s cause the detrending procedure to be executed on a set of only a few points. We found that a division into fewer than 65 data windows often causes the $F(q, s)$ curves to converge at the scale of saturation. Even small differences in realizations may cause drastic changes. The plots of $F(q, s)$ often show substantial fluctuations.

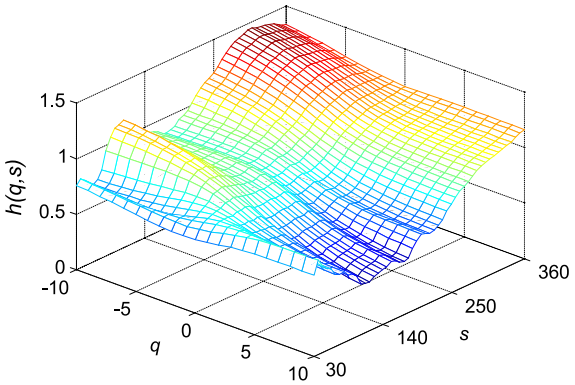

Fig. 14. Hurst surface $h(q, s)$ of rebar and wire rod warehouse-out quantity coupling multifractal among YZ, JS and BY warehouses.

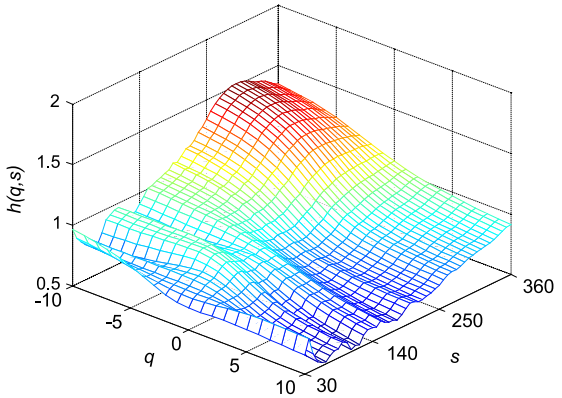

Fig. 15. Hurst surface $h(q, s)$ of wire rod warehouse-out quantity coupling multifractal among YZ, JS and BY warehouses.

6.2. Results of coupling multiscale multifractal surface

Fig. 14 shows that in a 6-sequence coupling system of both rebar and wire rod in warehouses, the generalized Hurst exponents will remain in a relatively high level no matter for large-scale fluctuation or small-scale fluctuation, when we set time scale at relatively high level. The Hurst exponent will attain a second peak when we set time scale around 90. Under small-scale fluctuation, the Hurst exponent will decrease as fluctuation increases.

Fig. 15 shows a 3-sequence coupling system of wire rod warehouse-out behavioral multifractal, with a single-peak Hurst surface. The peak is within the range of (250, 360) of time scale and $(-10, -5)$ of fluctuation. The Hurst exponents will decrease as the fluctuation increases or as time scale decreases.

Fig. 16 shows a 3-sequence coupling system of rebar warehouse-out behavioral multifractal, with a double-peak Hurst surface. With a relatively greater time scale, like (250, 360), the Hurst exponents remain at a high level, no matter for large-scale fluctuation or small-scale fluctuation, and will even tend to increase. The Hurst surface attains another peak at time scale of around 90, and the Hurst exponent will remain high under small-scale fluctuation, and tend to decrease under increasing fluctuation.

Fig. 17 shows a 3-sequence coupling system of steel warehouse-out behavioral multifractal, with a double-peak Hurst surface. With relatively large time scale like (250, 360) or time scale around 90, the Hurst exponents will decrease to lowest point as fluctuation increases.

7. Discussion

From comparison of Figs. 18 and 19, we found fat-tail probability distribution is the main source for coupling multifractal, no matter for rebar, wire rod or steel. The warehouse of JS ranked the top for contribution of coupling multifractal, followed by YZ and BY.

As for contribution of each product to coupling multifractal, we find that except for BY-Wire Rod, fat-tail probability distribution is the main cause of coupling multifractal.

Fig. 20 is the analysis result for 6-sequence coupling multifractal system and Fig. 20 also further verifies the results of Figs. 18 and 19. When considering long-term memory of rebar or wire rod, the ranks of warehouses are both JS, YZ and BY.

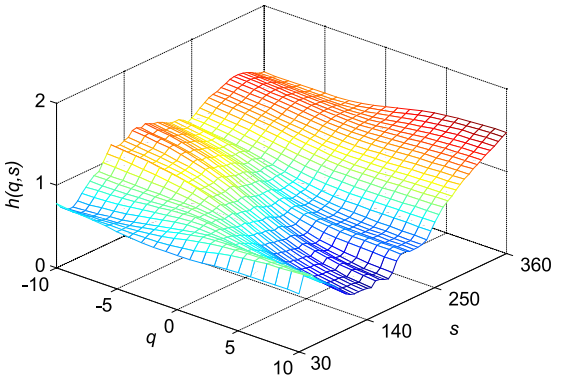

Fig. 16. Hurst surface $h(q, s)$ of rebar warehouse-out quantity coupling multifractal among YZ, JS and BY warehouses.

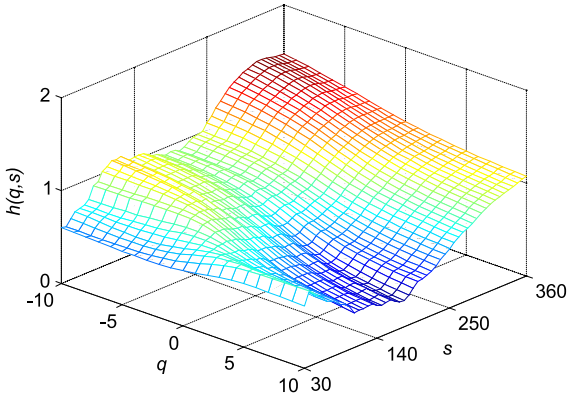

Fig. 17. Hurst surface $h(q, s)$ of total steel warehouse-out quantity coupling multifractal among YZ, JS and BY warehouses.

	1	2	3
	JS	YZ	BY
Fat-tail Distribution	High ↑	High ↑	Low ↓
Long-term Memory	Low ↑	Low ↑	High ↓

Fig. 18. Contribution of sources of wire rod of coupling multifractal in warehouses.

	1	2	3
	JS	YZ	BY
Fat-tail Distribution	High ↑	High ↑	High ↑
Long-term Memory	Low ↑	Low ↑	Low ↑

Fig. 19. Contribution of source of rebar of coupling multifractal in warehouses.

	1	2	3	4	5	6
Long-term Memory	JS-Wire Rod	JS-Rebar	YZ- Rebar	BY- Rebar	YZ-Wire Rod	BY-Wire Rod
Fat-tail Distribution	JS-Rebar	JS-Wire Rod	BY-Wire Rod	YZ-Wire Rod	YZ- Rebar	BY- Rebar

Fig. 20. Contribution of source of rebar and wire rod of coupling multifractal in warehouses.

Additionally, Fig. 20 also ranks all six warehouse-product combinations; i.e. when only considering long-term memory, the rank of combinations is JS-Wire Rod, JS-Rebar, YZ-Rebar, BY-Rebar, YZ-Wire Rod and BY-Wire Rod.

Analysis of multiscale multifractal surface reveals that the characteristics of coupling multifractal have something to do with time scale range; specifically, higher value of time scale like (250, 360) will respond to higher coupling multifractal strength. Except for the surface of wire rod 3-sequence coupling multifractal, the other three surfaces of rebar 3-sequence coupling multifractal, steel 3-sequence coupling multifractal and wire rod-rebar 6-sequence coupling multifractal follow double-peak property. And when the time scale is set around 90, Hurst exponents will significantly decrease as the fluctuation increases.

8. Conclusion

Based on multiple-sequence coupling multifractal framework, this paper extends the study of warehouse-out behaviors from single sequence multifractal based on R/S [7], double-sequence cross-correlation multifractal based on MF-DCCA and MF-DMA [8] to multiple sequence coupling multifractal analysis. Results show that from perspectives of products, warehouse-out behaviors among JS, YZ and BY warehouses follow coupling multifractal features, no matter for rebar or wire rod product, revealing that the long-term memory of a given warehouse-out behaviors can affect behaviors of other units.

Further, to figure out the source of coupling multifractal, we focus on warehouse-out behaviors of a given product, compare the contribution of fat-tail distribution and long-term memory on coupling multifractal among behaviors of warehouses and reveal dynamics regulation of various warehouse-product combinations. As for contribution of different warehouses, we find fat-tail probability is the main source, no matter for any product; as for the rank of warehouse based on contribution to coupling multifractal, JS rank the top, followed by YZ and BY. Specifically, JS-rebar and JS-wire rod combinations are the most influential than other warehouse-product combinations, no matter from long-term memory or fat-tail distribution. From perspective of product, the long-term memory of rebar will be more influential than that of wire rod.

Finally, based on MMA algorithm, we propose surfaces of generalized exponents incorporating fluctuation and time scale simultaneously, and detect the dynamics regulation of steel 3-sequence system, rebar 3-sequence system, wire rod 3-sequence system and rebar–wire rod 6-sequence system.

Acknowledgments

This research was supported by the National Natural Science Foundation of China (Grant 71201060), Research Fund for the Doctoral Program of Higher Education (Grant 20120172120051), and the Fundamental Research Funds for the Central Universities (Grants 2015ZZ059, 2015ZDXM04).

References

[1] A.L. Barabsi, The origin of bursts and heavy tails in human dynamics, Nature 435 (7039) (2005) 207–211.
[2] M.C. Gonzlez, C.A. Hidalgo, A.L. Barabsi, Understanding individual human mobility patterns, Nature 453 (7196) (2008) 779–782.
[3] A. Vzquez, J.G. Oliveira, Z. Dezs, K.-I. Goh, I. Kondor, A.-L. Barabsi, Modeling bursts and heavy tails in human dynamics, Phys. Rev. E 73 (036127) (2006) 80–98.
[4] P. Wang, T. Lei, H.Y. Chi, B. Wang, Heterogenous human dynamics in intra and inter-day time scale, Europhys. Lett. 94 (1) (2010) 18005–18009.
[5] A. Johansen, Probing human response times, Physica A 338 (12) (2004) 286–291.
[6] Z.Q. You, X.P. Han, L.Y. Lü, H.Y. Chi, Empirical studies on the network of social groups: The case of tencent qq, PLoS One 10 (7) (2014) e0130538.
[7] C.Z. Yao, J.N. Lin, X.F. Liu, X.Z. Zheng, Dynamic features analysis for the large-scale logistics system warehouse-out operation, Physica A 415 (2014) 31–42.
[8] C. Yao, J. Lin, X. Zheng, Multifractal detrended cross-correlation analysis for large-scale warehouse-out behaviors, Fractals 23 (4) (2015) 1550044.
[9] W.X. Zhou, The components of empirical multifractality in financial returns, Europhys. Lett. 88 (2) (2009) 28004.
[10] W.X. Zhou, Finite-size effect and the components of multifractality in financial volatility, Chaos Solitons Fractals 45 (2) (2012) 147155.
[11] C.K. Peng, S.V. Buldyrev, S. Havlin, M. Simons, H.E. Stanley, A.L. Goldberger, Mosaic organization of dna nucleotides, Phys. Rev. E 49 (2) (1994) 1685–1689.
[12] J.W. Kantelhardt, S.A. Zschiegner, E. Koscielny-Bunde, S. Havlin, A. Bunde, H.E. Stanley, Multifractal detrended fluctuation analysis of nonstationary time series, Physica A 316 (1–4) (2002) 87–114.
[13] R. Hasan, S.M. Mohammad, Multifractal analysis of asian markets during 20072008 financial crisis, Physica A 419 (2015) 746–761.
[14] Z. Li, X. Lu, Multifractal analysis of China's agricultural commodity futures markets, Energy Procedia 5 (2011) 1920–1926.
[15] J. Qin, X. Lu, Y. Zhou, L. Qu, The effectiveness of China's rmb exchange rate reforms: An insight from multifractal detrended fluctuation analysis, Physica A 421 (2015) 443–454.
[16] R. Gu, H. Chen, Y. Wang, Multifractal analysis on international crude oil markets based on the multifractal detrended fluctuation analysis, Physica A 389 (14) (2010) 2805–2815.
[17] Calvet Laurent, Multifractality in asset returns: theory and evidence, Rev. Econ. Stat. 84 (3) (2002) 381–406.
[18] B. Podobnik, H.E. Stanley, Detrended cross-correlation analysis: a new method for analyzing two nonstationary time series, Phys. Rev. Lett. 100 (8) (2007) 38–71.
[19] W.X. Zhou, Multifractal detrended cross-correlation analysis for two nonstationary signals, Phys. Rev. E 77 (6) (2008) 066211.
[20] C. Meneveau, K.R. Sreenivasan, P. Kailasnath, M.S. Fan, Joint multifractal measures: Theory and applications to turbulence, Phys. Rev. A 41 (2) (1990) 894–913.
[21] J. Wang, P. Shang, W. Ge, Multifractal cross-correlation analysis based on statistical moments, Fractals 20 (03n04) (2011) 271–279.
[22] W.J. Xie, Z.Q. Jiang, G.F. Gu, X. Xiong, W.X. Zhou, Joint multifractal analysis based on the partition function approach: Analytical analysis, numerical simulation and empirical application, New J. Phys. 17 (10) (2015) 27–30.

[23] P. Owieimka, S. Drod, M. Forczek, S. Jadach, J. Kwapie, Detrended cross-correlation analysis consistently extended to multifractality, Phys. Rev. E 89 (2) (2014) 023305.
[24] X.Y. Qian, Y.M. Liu, Z.Q. Jiang, B. Podobnik, W.X. Zhou, H.E. Stanley, Detrended partial cross-correlation analysis of two nonstationary time series influenced by common external forces, Phys. Rev. E 91 (6) (2015) 62816.
[25] G.F. Zebende, Dcca cross-correlation coefficient: Quantifying level of cross-correlation, Physica A 390 (390) (2011) 614–618.
[26] J. Kwapie, P. Owicimka, S. Drod, Detrended fluctuation analysis made flexible to detect range of cross-correlated fluctuations, Phys. Rev. E 92 (5–1) (2015) 052815.
[27] R. Balocchi, M. Varanini, A. Macerata, Quantifying different degrees of coupling in detrended cross-correlation analysis, Europhys. Lett. 101 (2) (2013) 20011.
[28] L. Kristoufek, Measuring correlations between non-stationary series with dcca coefficient, Physica A 402 (10) (2014) 291–298.
[29] L. Kristoufek, Detrending moving-average cross-correlation coefficient: Measuring cross-correlations between non-stationary series, Physica A 406 (10) (2013) 169–175.
[30] L. Kristoufek, Detrended fluctuation analysis as a regression framework: estimating dependence at different scales, Phys. Rev. E 91 (2) (2015) 022802.
[31] E. Alessio, A. Carbone, G. Castelli, V. Frappietro, Second-order moving average and scaling of stochastic time series, Eur. Phys. J. B 27 (2) (2002) 197–200.
[32] G.-F. Gu, W.-X. Zhou, Detrending moving average algorithm for multifractals, Phys. Rev. E 82 (2010) 011136.
[33] Z.Q. Jiang, W.X. Zhou, Multifractal detrending moving-average cross-correlation analysis, Phys. Rev. E 84 (2) (2011) 664–675.
[34] L. Kristoufek, Multifractal height cross-correlation analysis: A new method for analyzing long-range cross-correlations, Quant. Finance 95 (6) (2011) 525–604.
[35] J. Gieratowski, J.J. Żebrowski, R. Baranowski, Multiscale multifractal analysis of heart rate variability recordings with a large number of occurrences of arrhythmia, Phys. Rev. E 85 (2Pt1) (2012) 397–400.
[36] J. Gieratowski, D. Hoyer, F. Tetschke, Development of multiscale complexity and multifractality of fetal heart rate variability, Auton. Neurosci.-Basic Clin. 178 (1–2) (2013) 29–36.
[37] J. Wang, P. Shang, X. Cui, Multiscale multifractal analysis of traffic signals to uncover richer structures, Phys. Rev. E 89 (3) (2014) 032916.
[38] W. Shi, P. Shang, J. Wang, A. Lin, Multiscale multifractal detrended cross-correlation analysis of financial time series, Physica A 403 (6) (2014) 35–44.
[39] Y. Yin, P. Shang, Multiscale multifractal detrended cross-correlation analysis of traffic flow, Nonlinear Dynam. 81 (3) (2015) 1–19.
[40] A. Lin, H. Ma, P. Shang, The scaling properties of stock markets based on modified multiscale multifractal detrended fluctuation analysis, Physica A 436 (2015) 525–537.
[41] A. Lin, P. Shang, H. Zhou, Cross-correlations and structures of stock markets based on multiscale mf-dxa and pca, Nonlinear Dynam. 78 (1) (2014) 485–494.
[42] L. Hedayatifar, M. Vahabi, G.R. Jafari, Coupling detrended fluctuation analysis for analyzing coupled nonstationary signals, Phys. Rev. E 84 (1) (2011) 1572–1586.
[43] S. Shadkhoo, G.R. Jafari, Multifractal detrended cross-correlation analysis of temporal and spatial seismic data, Phys.: Condens. Matter 72 (72) (2009) 679–683.
[44] G. Cao, J. Cao, L. Xu, Asymmetric multifractal scaling behavior in the Chinese stock market: Based on asymmetric mf-dfa, Physica A 392 (4) (2013) 797–807.
[45] M. Small, C.K. Tse, Detecting determinism in time series: The method of surrogate data, IEEE Trans. Circuits Syst. I, Fundam. Theory Appl. 50 (5) (2003) 663–672.